ICEE 2006 14th
Iranian Conference on Electrical Engineering

On the Effect of Scattering on the Performance of Carbon Nanotube Field-Effect Transistors

Mahdi Pourfath, Hans Kosina, and Siegfried Selberherr
Institute for Microelectronics, Technische Universität Wien
Gußhausstraße 27-29, A-1040 Vienna, Austria
pourfath@iue.tuwien.ac.at

Abstract

Based on the non-equilibrium Green's function formalism the performance of carbon nanotube field-effect transistors has been studied. The effects of elastic and inelastic scattering on the device performance have been investigated. The results indicate that elastic scattering has a more detrimental effect on the device characteristics than inelastic scattering. Only for short devices the performance is not affected because of the long mean free path for elastic scattering.

1. Introduction

A carbon nanotube (CNT) can be viewed as a rolled-up sheet of graphite with a diameter of a few nano-meters. Depending on the chiral angle the CNT can be either metallic or semiconducting [1]. Semiconducting CNTs can be used as channels for field-effect transistors (FETs). CNTFETs have been studied in recent years as potential alternatives to CMOS devices because of their capability of ballistic transport. While early devices have shown poor device characteristics, high performance devices were achieved recently [2–6].

Depending on the work function difference between the metal contact and the CNT, carriers at the metal-CNT interface encounter different barrier heights. Devices with positive (Schottky type) [7, 8] and zero (ohmic) [9] barrier heights were fabricated. Devices with positive barrier heights have lower I_{on} and also suffer from ambipolar behavior [10–12], while devices with zero barrier height theoretically [13] and experimentally [3] show better performance. In this work we focus on devices with zero barrier height for electrons. The barrier height for holes is given by the band gap of the CNT.

Using the non-equilibrium Green's function (NEGF) formalism quantum phenomena like tunneling, and scattering processes can be rigorously modeled. The NEGF formalism has been successfully used to investigate the characteristics of nano-scale transistors [14, 15], CNTFETs [13, 16], and molecular transistors [17]. Recently a semiclassical Monte Carlo analysis of the effect of scattering on CNTFET characteristics has been reported [18, 19]. However, even with quantum corrections included, semiclassical methods cannot accurately predict the behavior of these devices because of the strong quantum effects. Therefore, in this work the NEGF formalism has been chosen to investigate transport phenomena in CNTFETs. The effect of elastic and inelastic scattering has been studied separately.

2. Approach

Due to quantum confinement along the tube circumference, wave function of carriers are bound around the CNT and can propagate along the tube axis. Assuming that the potential profile does not vary around the circumference of the CNT, sub-bands can be decoupled [15]. In this work we assume bias conditions in which the first sub-band contributes mostly to the total current. In the mode-space approach [15] the transport equations for each sub-band can be written as (1) and (2), see [20].

$$G^R = [EI - H - \Sigma^R_{\mathrm{el-ph}} - \Sigma^R_{\mathrm{s,d}}]^{-1} \tag{1}$$

$$G^{<,>} = G^R[\Sigma^{<,>}_{\mathrm{e-ph}}(E) + \Sigma^{<,>}_{\mathrm{s,d}}(E)]G^A \tag{2}$$

where $\Sigma^R_{\mathrm{e-ph}}$ is the self-energy due to electron-phonon interaction, $\Sigma^R_{\mathrm{s,d}}$ is the self-energy due to the coupling of the device to the source and drain contacts, which is only non-zero at the boundaries, and $G^A = [G^R]^\dagger$. A recursive Green's function method is used for solving (1) and (2), see [14]. In (1) an effective mass Hamiltonian is assumed, which is discretized using finite differences.

$$H = \begin{pmatrix} U_1 + 2t & -t & 0 & 0 & 0 & 0 & 0 \\ -t & U_2 + 2t & -t & 0 & 0 & 0 & 0 \\ 0 & \bullet & \bullet & \bullet & 0 & 0 & 0 \\ 0 & 0 & 0 & \bullet & \bullet & \bullet & 0 \\ 0 & 0 & 0 & 0 & -t & U_{n-1} + 2t & -t \\ 0 & 0 & 0 & 0 & 0 & -t & U_n + 2t \end{pmatrix} \tag{3}$$

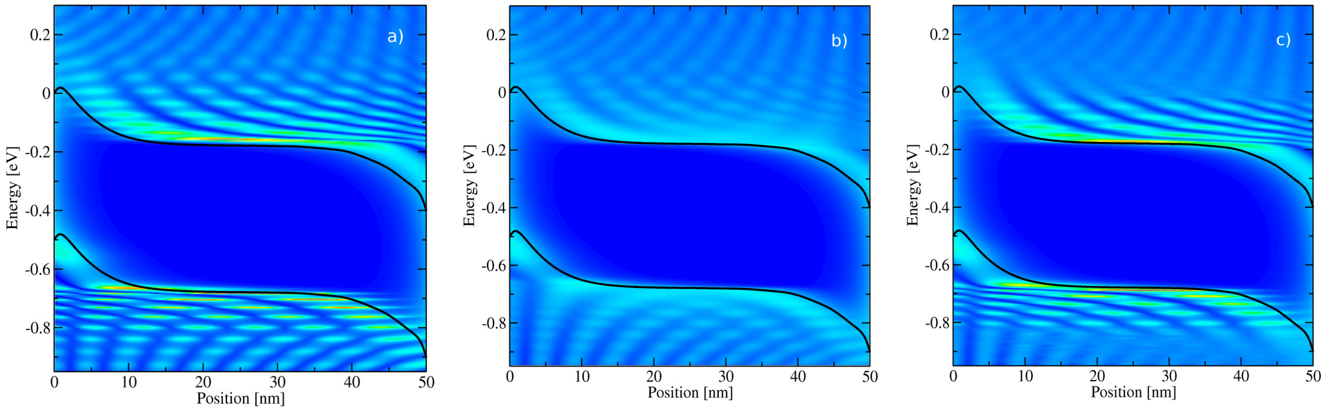

Figure 1. Local density of states for ballistic transport (a), with elastic scattering $\lambda_{\text{el}} = 10\ \text{nm}$ (b), and with inelastic scattering $\lambda_{\text{inel}} = 10\ \text{nm}$ (c).

Here U_j is the potential energy at the point j, $t = \frac{\hbar^2}{2m^*a^2}$, and a is the grid spacing. The self-energy due to electron-phonon interaction consists of the contribution of elastic and inelastic scattering mechanisms, $\Sigma^{<,>}_{\text{e-ph}} = \Sigma^{<,>}_{\text{el}} + \Sigma^{<,>}_{\text{inel}}$. Assuming a single sub-band the electron-phonon self-energies are simplified as (4)-(8).

$$\Sigma^{<,>}_{\text{el}}(E) = D_{\text{el}} G^{<,>}(E) \tag{4}$$

$$\begin{aligned}\Sigma^{<}_{\text{inel}}(E) = &\sum_{\nu} D_{\text{inel},\nu} \\ &[(n_B(\hbar\omega_\nu)+1)G^{<}(E+\hbar\omega_\nu) \\ &+n_B(\hbar\omega_\nu)G^{<}(E-\hbar\omega_\nu)]\end{aligned} \tag{5}$$

$$\begin{aligned}\Sigma^{>}_{\text{inel}}(E) = &\sum_{\nu} D_{\text{inel},\nu} \\ &[(n_B(\hbar\omega_\nu)+1)G^{>}(E-\hbar\omega_\nu) \\ &+n_B(\hbar\omega_\nu)G^{>}(E+\hbar\omega_\nu)]\end{aligned} \tag{6}$$

$$\Im m[\Sigma^{R}_{\text{e-ph}}(E)] = \frac{1}{2i}[\Sigma^{>}_{\text{e-ph}} - \Sigma^{<}_{\text{e-ph}}] \tag{7}$$

$$\Re e[\Sigma^{R}_{\text{e-ph}}(E)] = \frac{1}{\pi}\mathbf{P}\int \frac{\Im m[\Sigma^{R}_{\text{e-ph}}(E')]}{E'-E} dE' \tag{8}$$

where n_B is given by the Bose-Einstein distribution function:

$$n_B(\hbar\omega_\nu) = \frac{1}{\exp(\hbar\omega_\nu/k_B T) - 1} \tag{9}$$

Electron-phonon coupling constants, $D_{\text{el,inel}} \approx 1/\lambda_{\text{el,inel}}$, are chosen so as to satisfy experimentally measured values of the mean free path [16, 21, 22]. The mean free path of semiconducting CNTs at high energies approach those of metallic CNTs [18]. Reported values are $\lambda_{\text{el}} \approx 1.6\ \mu\text{m}$ and $\lambda_{\text{inel}} \approx 10\ \text{nm}$ for a metallic CNT with a diameter of 1.8nm [23]. Elastic scattering is due to acoustic phonons and inelastic scattering due to zone boundary and optical phonon modes with energies of $\hbar\omega_{\text{op}} = 160$ and $200\ \text{meV}$, respectively [23].

The transport equations are iterated to achieve convergence of the electron-phonon self-energies, resulting in a self-consistent Born approximation. The carrier concentration and the current density at some point j of the device can be calculated as (10) and (11).

$$n_j = -4i \int G^{<}_{j,j}(E) \frac{dE}{2\pi} \tag{10}$$

$$j_j = \frac{4q}{\hbar} \int 2Re\{G^{<}_{j,j+1}(E) H_{j+1,j}\} \frac{dE}{2\pi} \tag{11}$$

Carriers are treated as a sheet charge distributed over the surface of the CNT [25]. After convergence of the scattering self energies, the coupled system of the transport and Poisson equations is solved iteratively by using an appropriate numerical damping factor α, see Appendix. At the $(k+1)^{\text{th}}$ iteration the transport equation is solved using the electrostatic potential V^k from the last iteration and the new carrier concentration n^{k+1} is calculated. The Poisson equation is then solved by using n^{k+1} and an intermediate new electrostatic potential is calculated V^{k+1}_{int}. Finally $V^{k+1} = \alpha V^{k+1}_{\text{int}} + (1-\alpha)V^k$, where $0 < \alpha < 1$. Successive iteration continues until a convergence criterion is satisfied. In this work an adaptive damping factor was used. The damping factor is initially set to $\alpha = 1$. If the potential update $|V^{k+1} - V^k|$ increases from one iteration to the next iteration or remains constant the damping factor decreases by a constant factor.

The integration in (10) is calculated within an energy interval $[E_{\min}, E_{\max}]$. The interval can be simply divided into equidistant steps and the transport equation will be solved at these points. Using this method, narrow resonances at some

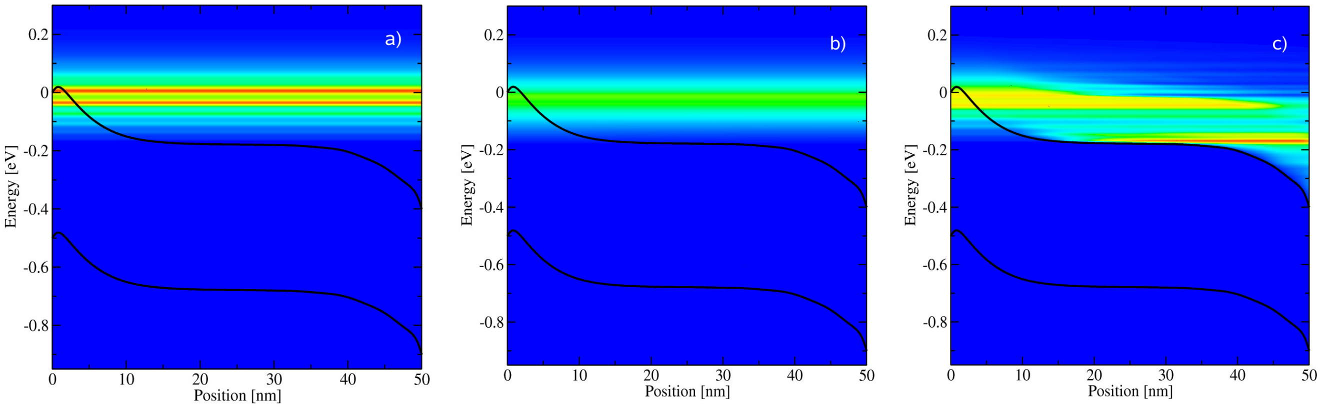

Figure 2. Current spectrum through the device for ballistic transport (a), with elastic scattering $\lambda_{\mathrm{el}} = 10\ \mathrm{nm}$ (b), and with inelastic scattering $\lambda_{\mathrm{inel}} = 10\ \mathrm{nm}$ (c).

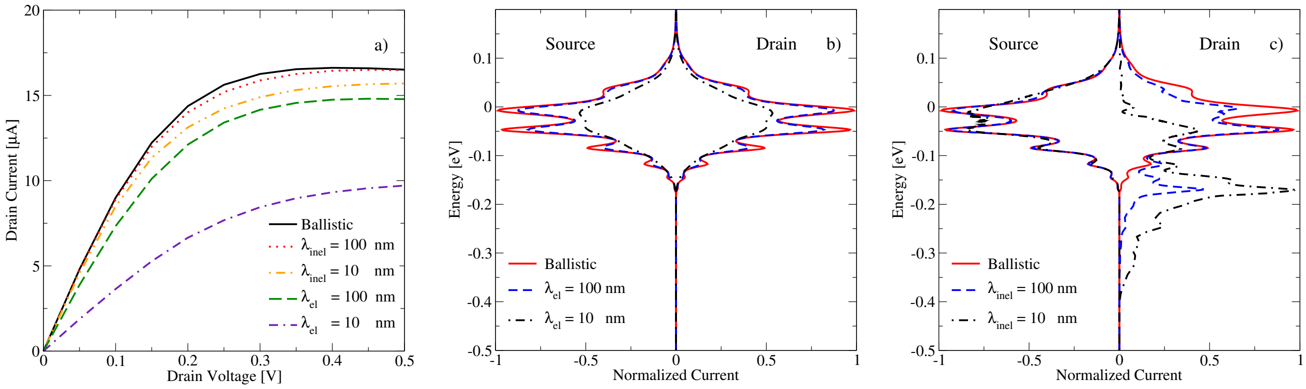

Figure 3. The effect of elastic and inelastic scattering on the output characteristic (a). The spectrum of the current by accounting for elastic (b), and inelastic scattering (c).

energies may be missed or may not be evaluated correctly. As the potential profile changes in successive iterations, the position of the resonances will also change, and it is possible that a resonance point locates very near to one of the energy steps. In this case the carrier concentration suddenly changes and as a result the simulation would oscillate and not converge. To avoid this problem the accuracy of the integration should be independent of the location of resonances. Using an adaptive integration method, the integrations in (10) can be evaluated with a desired accuracy and as result the self-consistent loop will be stable. Details are presented in [26].

3. Simulation Results and Discussions

First we investigate the effect of each scattering mechanism separately. Fig. 1 compares the normalized local density of states, defined as $\rho(\mathbf{r}, E) = i(G^{>}(\mathbf{r}, \mathbf{r}, E) - G^{<}(\mathbf{r}, \mathbf{r}, E))/2\pi$, for ballistic transport, with elastic and inelastic scattering. By including scattering the local density of states broadens and becomes more similar to its semi-classical counterpart. Fig. 1-c shows that inelastic scattering affects those electronic states in which carriers have enough kinetic energy to be scattered into lower energy states. Fig. 2 shows the normalized spectrum of the current for the aforementioned conditions. In all cases a large amount of current is delivered by tunneling. In the case of ballistic transport two peaks in the spectrum of the current are observed, the first one locates at the Fermi level of the source contact. The second one bellow the Fermi level is due to the formation of a localized state in the potential well close to the source contact. Scattering broadens the levels and as a result the peaks vanish. Elastic scattering conserves the energy of carriers as in the ballistic case, but the current decreases considerably due to the elastic back-scattering of carriers. On the other hand, with inelastic scattering the energy of carriers is not conserved. Carriers which acquire enough kinetic energy can emit phonons and scatter into lower energy states. This process does not decrease the current as much as elastic scattering does, since scattered car-

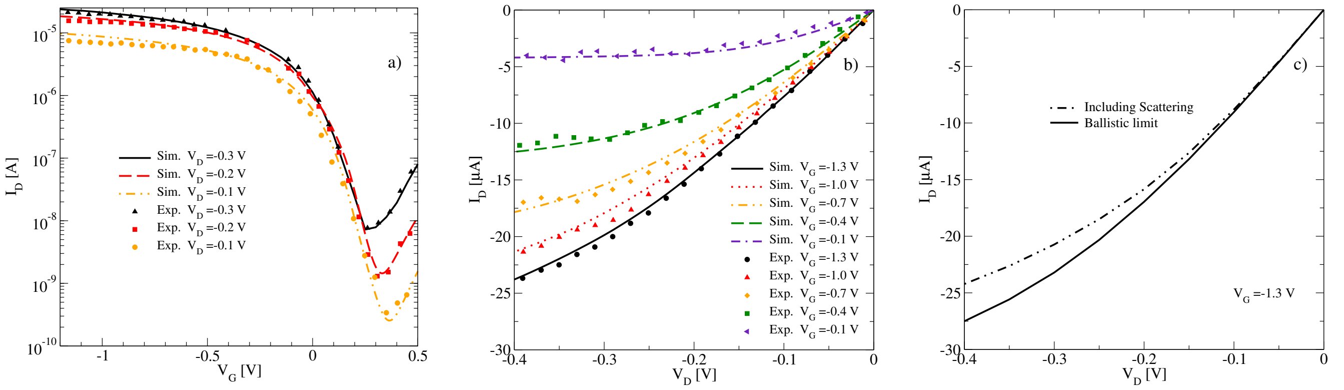

Figure 4. The comparison of the simulation results and experimental data for the transfer (a) and the output characteristic (b). Comparison of the output characteristic based on the ballistic transport and with scattering (c).

riers lose their kinetic energy and the probability for back-scattering is low [18]. For a better comparison Fig. 3-b, and Fig. 3-c show the spectra of the source and drain currents for these scattering mechanisms. When the mean free path for elastic scattering is decreased, the resonances in the current spectrum vanish (due to broadening) and the total current decreases considerably. When the mean free path for inelastic scattering is decreased, more carriers scatter from high energy states into lower energy states, and the shape of the source and drain current spectrum becomes asymmetric. Fig. 3-a shows that elastic scattering, unlike inelastic scattering, can severely degrade the on-current of the device.

For comparison with experimental data, we used the same material composition and geometrical parameters as reported in [3]. All our calculations assume a CNT with $E_g = 0.5$ eV, $m^* = 0.06 m_0$ [7] for both electrons and holes [1]. These parameters give excellent agreement between simulation and experimental data (Fig. 4). As shown in Fig. 4-c even at high bias condition the drain current is close to its ballistic limit.

4. Conclusions

We theoretically investigated the effect of scattering on the performance of CNTFETs. Due to strong quantum effects like tunneling, the NEGF is a very well suited method to study transport phenomena in such devices. Because of back-scattering, elastic scattering has a detrimental effect on the device performance. Due to a long mean free path for this process, the performance of short devices (less than several hundred nano-meter) is only weakly affected. On the other hand, the mean free path for inelastic scattering in CNTs is quite short, but this process does not degrade device performance. Our analysis shows that even in the presence of inelastic scattering, short CNTFETs can operate close to their ballistic limit.

5. Appendix

Block Diagram illustrating the iterative procedure to be followed in solving the coupled system of transport and Poisson equations.

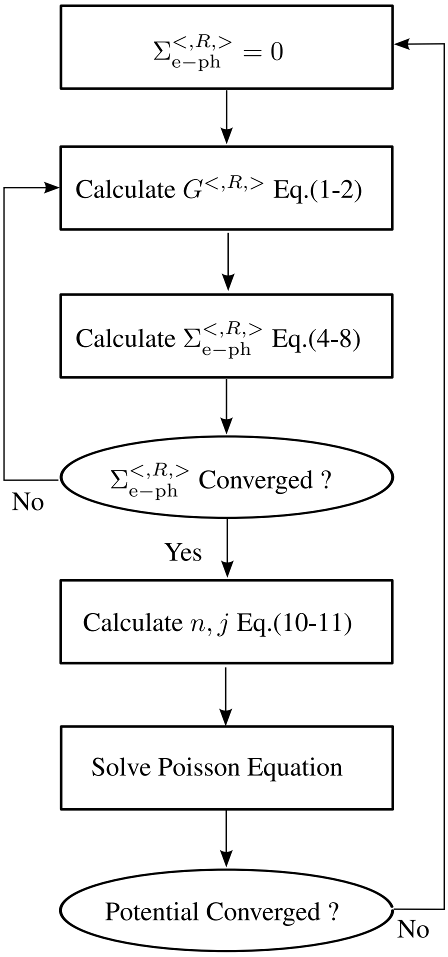

6. References

[1] R. Saito, G. D. Dresselhaus, and M. S. Dresselhaus, *Physical Properties of Carbon Nanotubes*. Imperial College Press, 1998.

[2] M. Radosavljevic, J. Appenzeller, P. Avouris, and J. Knoch, “High Performance of Potassium n-Doped Carbon Nanotube Field-Effect Transistors,” *Appl.Phys.Lett.*, vol. 84, no. 18, pp. 3693–3695, 2004.

[3] A. Javey, J. Guo, D. B. Farmer, Q. Wang, E. Yenilmez, R. G. Gordon, M. Lundstrom, and H. Dai, “Self-Aligned Ballistic Molecular Transistors and Electrically Parallel Nanotube Arrays,” *Nano Lett.*, vol. 4, no. 7, pp. 1319–1322, 2004.

[4] B. M. Kim, T. Brintlinger, E. Cobas, H. Zheng, M. Fuhrer, Z.Yu, R. Droopad, J. Ramdani, and K. Eisenbeiser, “High-Performance Carbon Nanotube Transistors on SrTiO3/Si Substrates,” *Appl.Phys.Lett.*, vol. 84, no. 11, pp. 1946–1948, 2004.

[5] A. Javey, R. Tu, D. B. Farmer, J. Guo, R. G. Gordon, and H. Dai, “High Performance n-Type Carbon Nanotube Field-Effect Transistors with Chemically Doped Contacts,” *Nano Lett.*, vol. 5, no. 2, pp. 345–348, 2005.

[6] P. Qi, A. Javey, M. Rolandi, Q. Wang, E. Yenilmez, and H. Dai, “Miniature Organic Transistors with Carbon Nanotubes as Quasi-One Dimensional Electrodes,” *J.Am.Chem.Soc.*, vol. 126, no. 38, pp. 11774–111775, 2004.

[7] J. Appenzeller, M. Radosavljevic, J. Knoch, and P. Avouris, “Tunneling Versus Thermionic Emission in One-Dimensional Semiconductors,” *Phys.Rev.Lett.*, vol. 92, p. 048301, 2004.

[8] S. Heinze, J. Tersoff, R. Martel, V. Derycke, J. Appenzeller, and P. Avouris, “Carbon Nanotubes as Schottky Barrier Transistors,” *Phys.Rev.Lett.*, vol. 89, p. 106801, 2002.

[9] A. Javey, J. Guo, Q. Wang, M. Lundstrom, and H. Dai, “Ballistic Carbon Nanotube Field-Effect Transistors,” *Letters to Nature*, vol. 424, no. 6949, pp. 654–657, 2003.

[10] M. Pourfath, A. Gehring, E. Ungersboeck, H. Kosina, S. Selberherr, B.-H. Cheong, and W. Park, “Separated carrier injection control in carbon nanotube field-effect transistors,” *J.Appl.Phys.*, vol. 97, pp. 1061031–1061033, 2005.

[11] M. Pourfath, E. Ungersboeck, A. Gehring, B. H. Cheong, W. Park, H. Kosina, and S. Selberherr, “Improving the Ambipolar Behavior of Schottky Barrier Carbon Nanotube Field Effect Transistors,” in *Proc. ESSDERC*, pp. 429–432, 2004.

[12] R. Martel, V. Derycke, C. Lavoie, J. Appenzeller, K. K. Chan, J. Tersoff, and P. Avouris, “Ambipolar Electrical Transport in Semiconducting Single-Wall Carbon Nanotubes,” *Phys.Rev.Lett.*, vol. 87, p. 256805, 2001.

[13] J. Guo, S. Datta, and M. Lundstrom, “A Numerical Study of Scaling Issues for Schottky Barrier Carbon Nanotube Transistors,” *IEEE Trans. Electron Devices*, vol. 51, no. 2, pp. 172–177, 2004.

[14] A. Svizhenko, M. Anantram, T. Govindan, B. Biegel, and R. Venugopal, “Two-Dimensional Quantum Mechanical Modeling of Nanotransistors,” *J.Appl.Phys.*, vol. 91, no. 4, pp. 2343–2354, 2002.

[15] R. Venugopal, Z. Ren, S. Datta, M. Lundstrom, and D. Jovanovic, “Simulating Quantum Transport in Nanoscale Transistors: Real versus Mode-Space Approaches,” *J.Appl.Phys.*, vol. 92, no. 7, pp. 3730–3739, 2002.

[16] A. Svizhenko and M. Anantram, “Effect of Scattering and Contacts on Current and Electrostatics in Carbon Nanotubes,” *cond-mat/0503769*, 2005.

[17] Y. Xue, S. Datta, and M. Ratner, “First-Principles Based Matrix Green’s Function Approach to Molecular Electronic Devices: General Formalism,” *Chemical Physics*, vol. 281, no. 2-3, pp. 151–170, 2002.

[18] J. Guo and M. Lundstrom, “Role of phonon scattering in carbon nanotube field-effect transistors,” *Appl.Phys.Lett.*, vol. 86, p. 193103, 2005.

[19] S. Hasan, J. Guo, M. Vaidyanathan, and M. Lundstrom, “Monte-Carlo Simulation of Carbon Nanotube Devices,” *J.Comp.Electronics*, vol. 3, no. 3-4, pp. 333–336, 2005.

[20] S. Datta, *Electronic Transport in Mesoscopic Systems*. Cambridge University Press, 1995.

[21] J. Guo, “A Quantum-Mechanical Treatment of Phonon Scattering in Carbon Nanotube Transistors,” *J.Appl.Phys.*, vol. 98, p. 063519, 2005.

[22] S. Koswatta, M. Lundstrom. “Simulation of Phonon-Assisted Band-to-Band Tunneling in Carbon Nanotube Field-Effect Transistors,” *Appl.Phys.Lett.*, vol. 87, p. 253107, 2005.

[23] J. Park, S. Rosenblatt, Y. Yaish, V. Sazonova, H. Ustunel, S. Braig, T. Arias, P. Brouwer, and P. McEuen, “Electron-Phonon Scattering in Metallic Single-Walled Carbon Nanotubes,” *Nano Lett.*, vol. 4, no. 3, pp. 517–520, 2004.

[24] G. Pennington and N. Goldsman, “Semiclassical Transport and Phonon Scattering of Electrons in Semiconducting Carbon Nanotubes,” *Phys.Rev.B*, vol. 68, p. 045426, 2003.

[25] M. Pourfath, E. Ungersboeck, A. Gehring, W. J. Park, B. H. Cheong, H. Kosina, and S. Selberherr, “Optimization of Schottky Barrier Carbon Nanotube Field Effect Transistors,” *Microelectronic Engineering*, vol. 81, no. 2-4, pp. 428–433.

[26] M. Pourfath, H. Kosina, and S. Selberherr, “A Fast and Stable Poisson-Schrödinger Solver for the Analysis of Carbon Nanotube Transistors,” *accepted in J.Comp.Electronics*, 2006.